Simulation of DC Helicity Injection and Energy Confinement in the SSPX Spheromak

Carl Sovinec and Giovanni Cone

University of Wisconsin-Madison

and

Bruce Cohen

Lawrence Livermore National Laboratory

Joint NSTX/Theory Seminar, July 1, 2004

Princeton Plasma Physics Laboratory

Outline

- Introduction
  - Spheromak background
  - Need for simulation
- Summary of 0-*b* results
- SSPX modeling
  - Parameters of the computations
  - Comparison with SSPX results
  - Four stages of simulated evolution
  - Energy transport
- Discussion and Conclusions

The most successful spheromak formation scheme uses electrodes impregnated with vacuum poloidal flux.

- Slow formation was a major conceptual breakthrough [Jarboe, *et al.*, PRL **51**, 39 (1983)].
- Most theoretical descriptions have been based on relaxation arguments [Taylor, PRL **33**, 1139 (1974); Jarboe, PPCF **36**, 945 (1994)].
  - No information on fluctuations
  - Sustainment described by global helicity balance and cascades
- During drive, T_e<50 eV, but during decay or partial drive, T_e >>100 eV has been recorded.

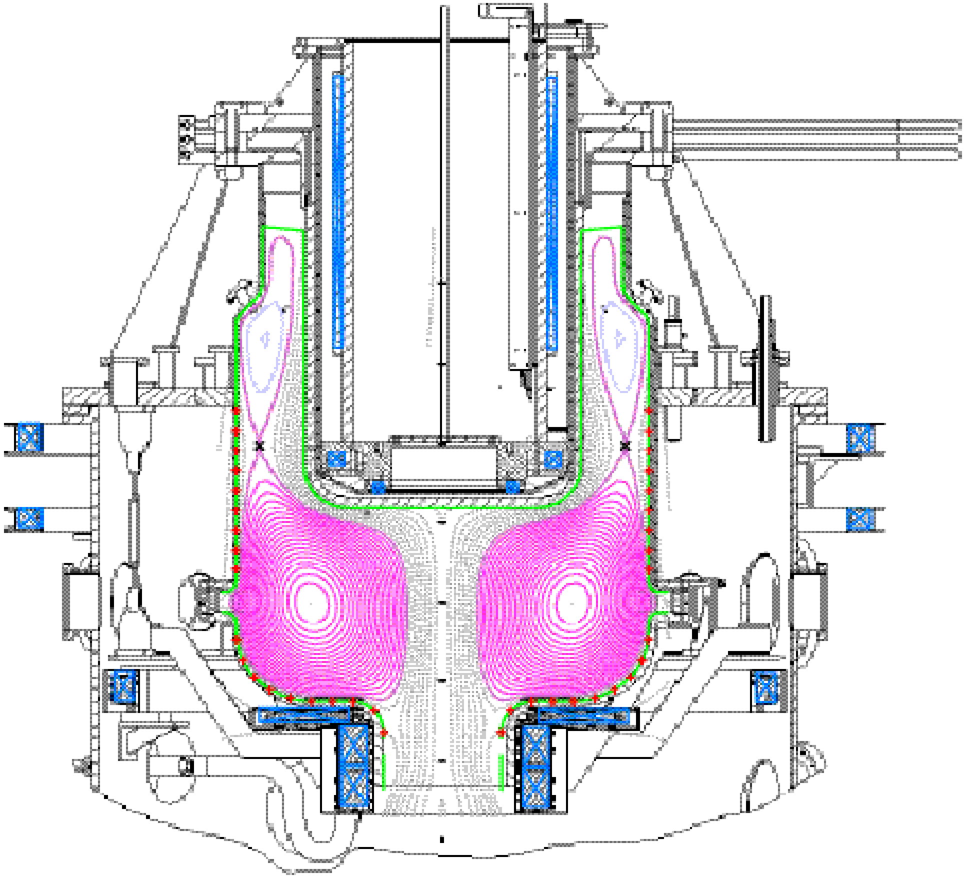

Schematic of the SSPX spheromak experiment at LLNL with contours of reconstructed symmetric poloidal flux.

While relaxation theory provides insight, numerical computation is required to solve the time-dependent nonlinear equations that describe macroscopic evolution.

- The first numerical MHD studies investigated nonlinear behavior during decay from a symmetric spheromak. [Katayama and Katsurai, Phys. Fluids **29**, 1939 (1986), Sgro, Mirin, and Marklin, Phys. Fluids **30**, 3219 (1987), and Horiuchi, Sato, and Uchida, Phys. Fluids B **4,** 672 (1992).]
- Simulations of generic spheromaks at 0-*b* addressed MHD activity underlying formation and sustainment [Finn, PRL **85**, 4538 (2000), Sovinec, Phys. Plasmas **8**, 475 (2001)].
  - Flux amplification results from n=1 MHD activity.
  - Average parallel current is flattened by a dynamo effect.
  - Chaotic scattering of field-lines occurs during sustainment.
  - Closed flux surfaces form during decay.
  - Confinement was not addressed directly.

Recent computations evolve temperature and number density, in addition to the basic resistive MHD model, to investigate energy confinement properties.

$$\frac{\partial \mathbf{B}}{\partial t} = \nabla \times \left(\mathbf{V} \times \mathbf{B} - h\mathbf{J} \right)$$ Faraday's/Ohm's laws

$$m_0 \mathbf{J} = \nabla \times \mathbf{B}$$ low-w Ampere's law

$$r\left(\frac{\partial \mathbf{V}}{\partial t} + \mathbf{V} \cdot \nabla \mathbf{V} \right) = \mathbf{J} \times \mathbf{B} - \nabla p + \nabla \cdot n r \nabla \mathbf{V}$$ flow evolution

$$\frac{\partial n}{\partial t} + \nabla \cdot \left(n\mathbf{V} \right) = \nabla \cdot D \nabla n$$ particle continuity

$$\frac{n}{g - 1}\left(\frac{\partial T}{\partial t} + \mathbf{V} \cdot \nabla T \right) = -\frac{p}{2} \nabla \cdot \mathbf{V} + \nabla \cdot n\left[c_{\|} \hat{\mathbf{b}}\hat{\mathbf{b}} + c_{\perp}\left(\mathbf{I} - \hat{\mathbf{b}}\hat{\mathbf{b}} \right) \right] + \frac{h\mathbf{J}^2}{2}$$ (single) temperature evolution

$$\hat{\mathbf{b}} \equiv \mathbf{B} / \left| \mathbf{B} \right|$$ local magnetic direction vector

- Braginskii transport coefficients are used for $c_{\|}$ (electron), $c_{\perp}$ (ion), and h.
- Heating is Ohmic.
- The NIMROD code [http://nimrodteam.org] evolves the system in 3D.
    - High-order finite elements help resolve anisotropies [JCP **195**, 355 (2004)].

Earlier 0-*b* MHD Simulation Results

- Nonlinear effects from saturation of the n=1 lead to formation and sustainment.
  - poloidal flux amplification (conversion from toroidal flux)
  - parallel current profile is relaxed
  - MHD dynamo effect sustains toroidal current
  - symmetry-breaking leaves **B** chaotic in most sustained conditions
- There are four different classes of nonlinear states in an *S*-Voltage phase diagram.
- Closed flux surfaces with net current form during decay.
- Related numerical studies include:
  - DC injection in RFPs: [Ho, NF **31**, 341 (1991); Sovinec, PhD dissertation, UW (1995)]
  - Solar physics: [Lau, PoP **3**, 3983 (1996); Lionello, PoP **5**, 3722 (1998)]
  - Tokamak current drive: [Sovinec, PoP **3**, 1038 (1996); Tang, PoP **11**, 2679 (2004)]

Three-dimensional computations in can and gun-driven configurations reproduce flux amplification/spheromak formation.

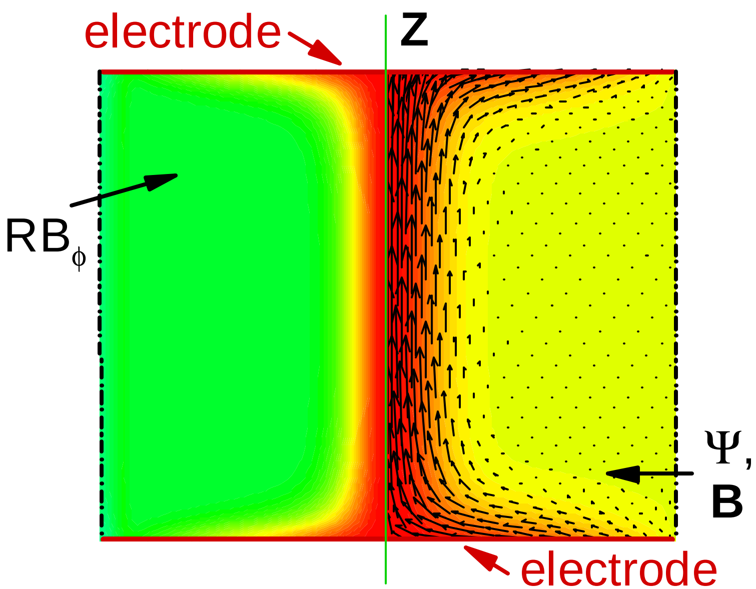

Two-dimensional computations in a can geometry show pinching only.

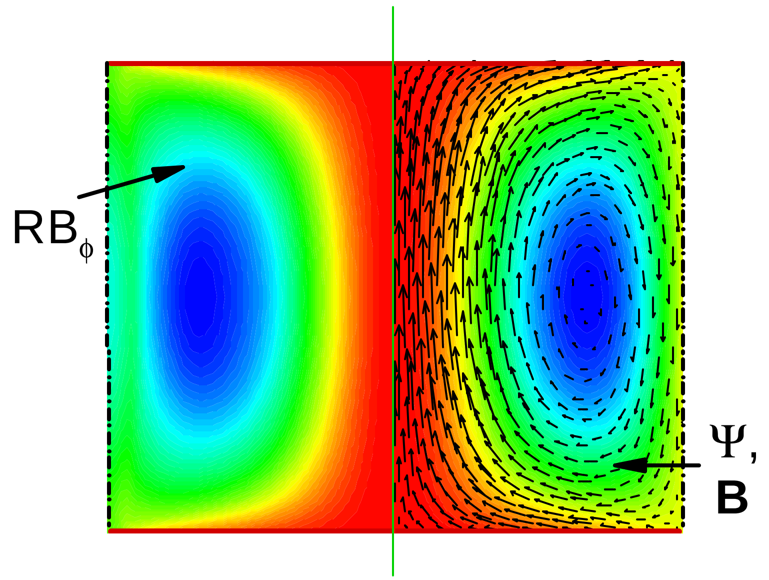

MHD activity in 3D computations reproduce amplification of the *symmetric* poloidal flux (Ψ_0).

Saturation of the n=1 leads to several important effects in addition to poloidal flux amplification.

1) The symmetric projection of parallel current density ($\mu_0 a\mathbf{J}\cdot\mathbf{B}/B^2$) is distributed throughout the volume (relaxation).

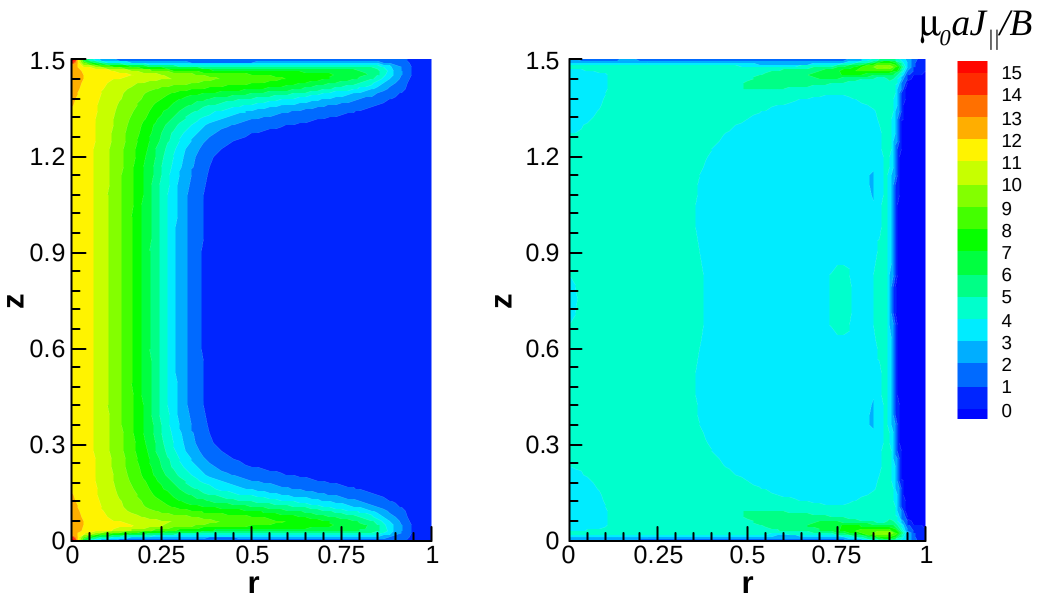

Before saturation. **After saturation.**

Examining 3D distributions, the parallel current density is carried by a helical current channel, reminiscent of the "doughhook" observed in SPHEX. [Duck, PPCF **39**, 715 (1997).]

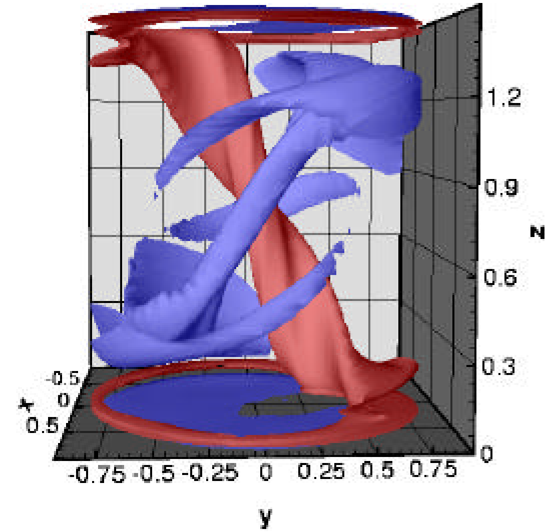

Effects from Saturation, Continued

2) When sustained, the fluctuations generate MHD dynamo effects that maintain toroidal current against resistive dissipation.

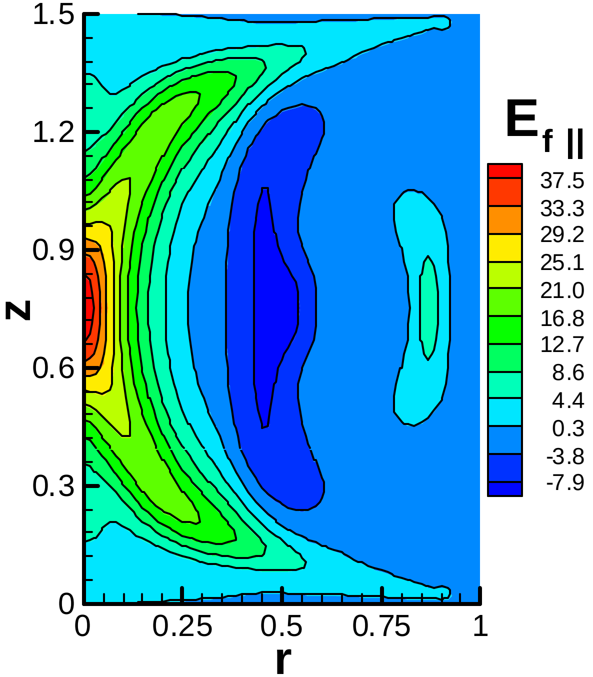

$\mathbf{E}_{f\|} \equiv \langle -\mathbf{v}_n{}' \mathbf{b}_n \rangle_{\|}$ from n=1

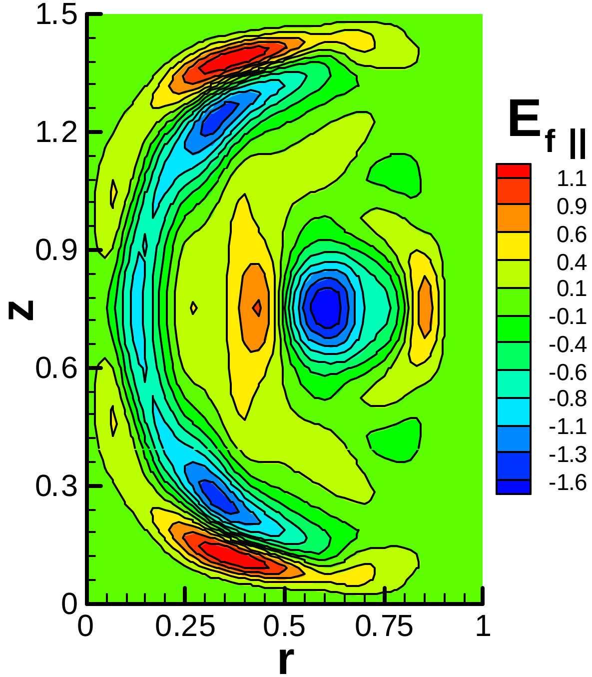

$\langle -\mathbf{v}_n{}' \mathbf{b}_n \rangle_{\|}$ from n=2

- Dynamo was measured in SPHEX, each *n* was thought to represent separate activity [al-Karkhy, *et al.*, PRL **70,** 1814 (1993).
- NIMROD simulations show n>1 to be nonlinearly generated by n=1 during sustainment.

Effects from Saturation, Continued

3) As the MHD fluctuations reconnect **B**-field and break the toroidal symmetric of the pinched open-field current column, they ensnarl magnetic field lines throughout the volume.

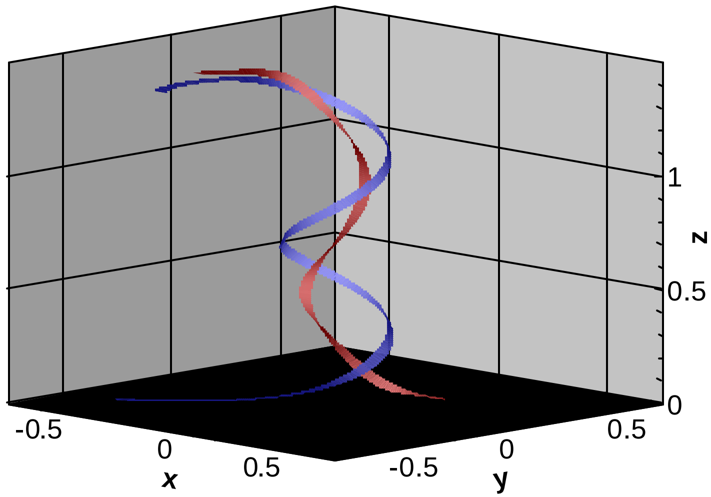

B-field traces before saturation.

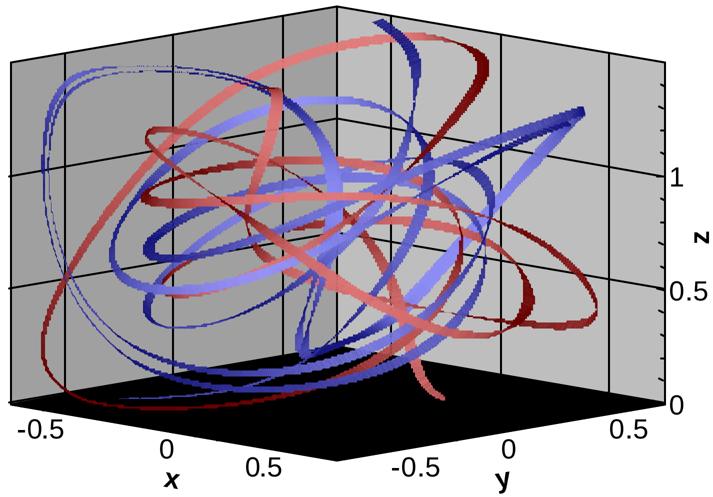

B-field traces after saturation.

- The entanglement and reconnection of injected toroidal flux with the bias poloidal flux leads to poloidal flux amplification.

- There is some confinement on the open fields (discussed later).

Nonlinear behavior at different sustained voltages and resistivity values can be summarized in a phase diagram.

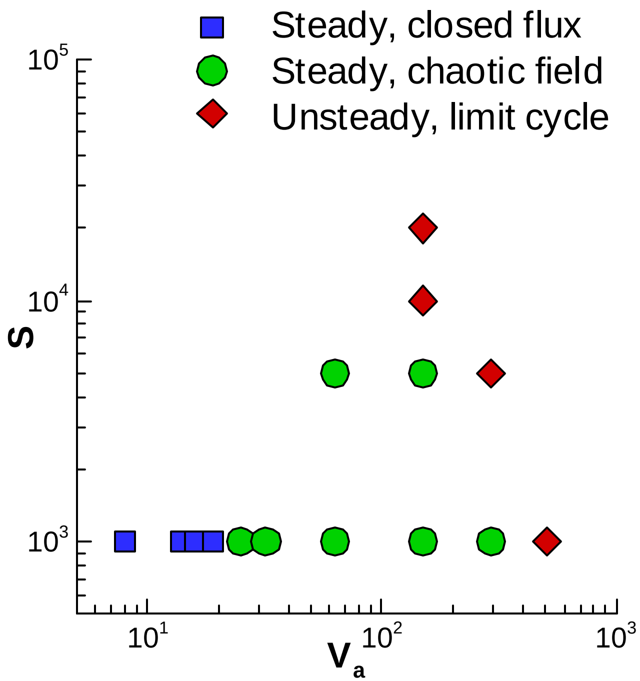

Phase diagram of "can" results. Symmetric state exists at low S, V_a.

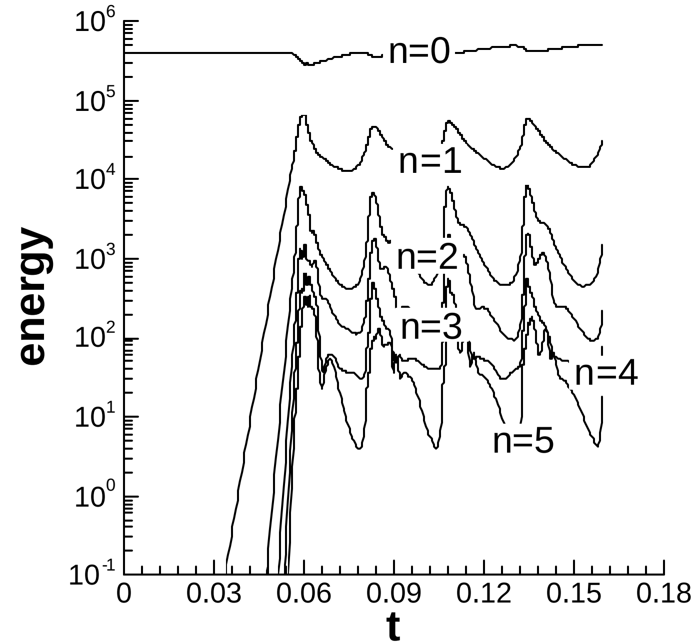

Limit cycle behavior of magnetic fluctuation energies in a sustained "can" configuration at S=5000.

$$\left[V_a \equiv \frac{t_r \int \mathbf{E}_a \cdot d\boldsymbol{L}}{\Psi_e} \right] \qquad S \equiv \frac{t_r}{t_A}$$

<u>When drive is removed from sustained conditions, closed flux surfaces often form.</u>

• Magnetic fluctuations decay faster than the mean poloidal flux generated by the flux conversion.

• Slow decay of mean poloidal flux acts as an Ohmic drive for toroidal current on the flux surfaces.

• These combined transient effects were proposed as the reason underlying temperature increases during decay in experiments [PoP **8**, 475 (2002)].

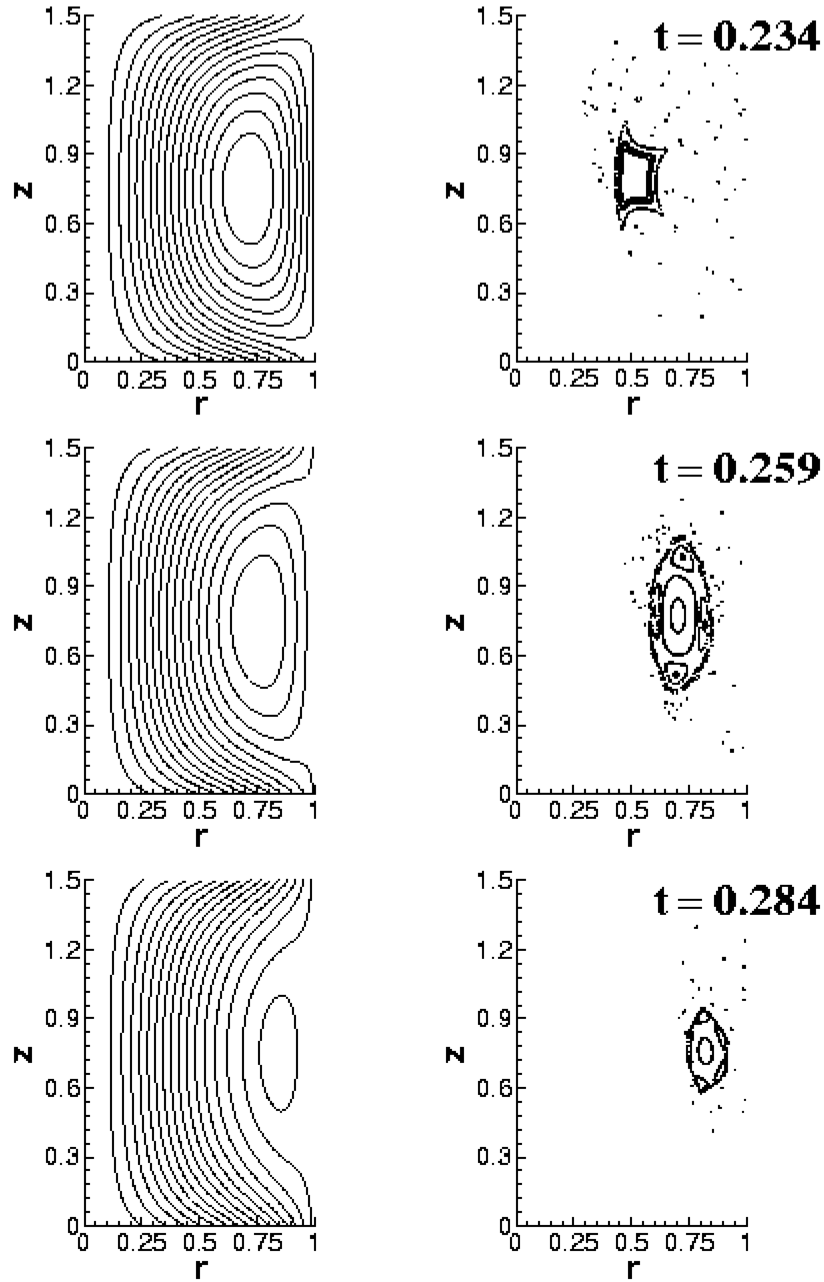

Simulation of SSPX 4620-4644 Shot Series

INPUT (Collisional coefficients are based on Hydrogen and Z=1):

- $n = 5\times10^{19}\ \mathrm{m}^{-3}$
- $\dfrac{h(T)}{m_0} = 411\left(\dfrac{1\,\mathrm{eV}}{T}\right)^{3/2}\ \mathrm{m}^2/\mathrm{s}$
- $c_\parallel(T) = 387\left(\dfrac{T}{1\,\mathrm{eV}}\right)^{5/2}\ \mathrm{m}^2/\mathrm{s}$
- $c_\perp = 0.50\left(\dfrac{1\,\mathrm{eV}}{T}\right)^{1/2}\left(\dfrac{1\,\mathrm{T}}{B}\right)^{2}\ \mathrm{m}^2/\mathrm{s}$
- $T_{wall} = 0.1\ \mathrm{eV}$
- y_{vacuum} specified
- $I_{\mathrm{inj}}(t)$ via boundary conditions on **B**
- Heat sink controls boundary layer
- $n = D = 2000\ \mathrm{m}^2/\mathrm{s}$

OUTPUT: Everything else

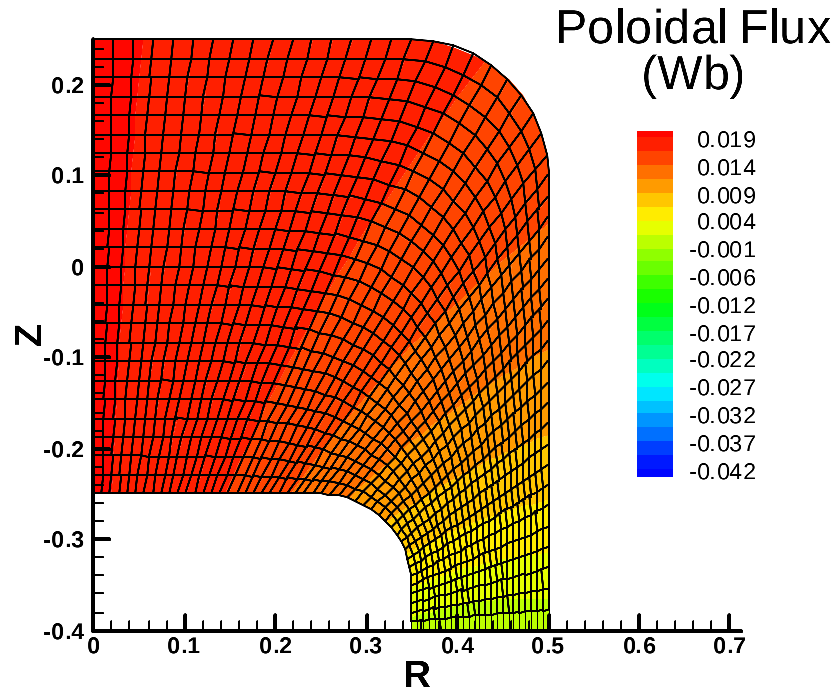

Initial (vacuum) poloidal flux distribution and the NIMROD mesh of bicubic finite elements representing SSPX (upside down).

- $0 \le n \le 2$ and $0 \le n \le 5$ Fourier comps. in f

Validity of Collisional Transport

- 0-*b* MHD results suggest that open-field transport governs confinement during driven conditions.
  - Collisional 3D transport modeling is appropriate for a chaotic **B** topologies if the effective mean-free-path is sufficiently small.
  - We can confirm *a posteriori* that collisionless conditions only exist when and where closed flux surfaces form.
- At n=5×10^{19} m^{-3} and T=1 eV,

$v_{Te} \cong 6\times10^{5}$ m/s

$t_e \cong 7\times10^{-10}$ s

$l_e \cong 4\times10^{-4}$ m $<< L$

- Scaling l_e with T^2 indicates that l_e reaches the chamber radius at approximately 35 eV.
- From this we infer that anisotropic thermal conduction is a good model for sustained (open field) conditions and for the transition to closed flux during decay.

Comparison of Numerical and Experimental Results

The simulated injector current is programmed to approximate the series of SSPX discharges reported in [McLean, *et al.*, PRL **88**, 125004-1 (2002)].

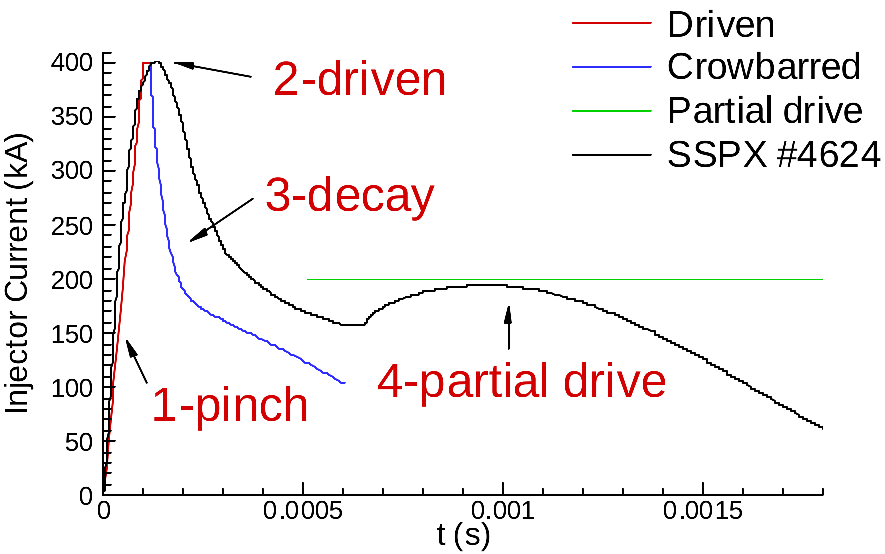

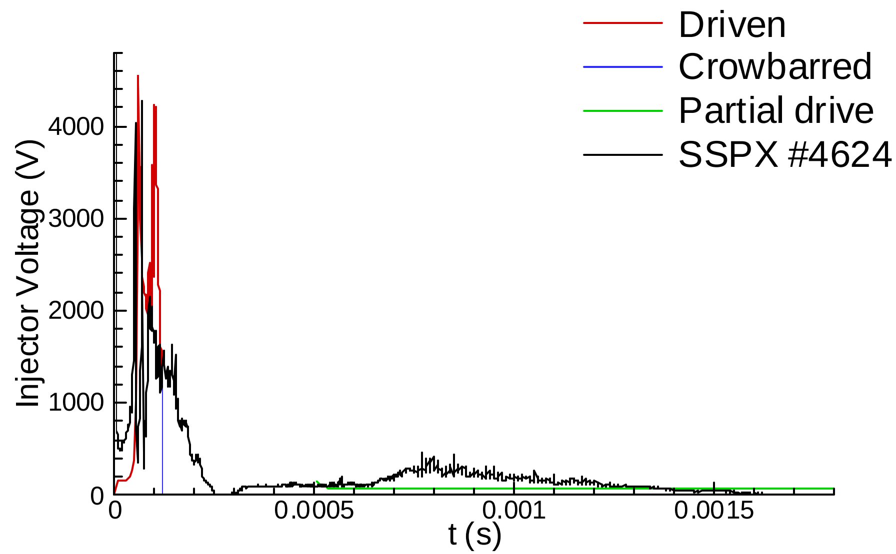

A strongly driven phase is followed by decay and then a second, partial drive. [SSPX Data courtesy of H. S. McLean.]

In the early driven phase, the applied potential reaches a few kV. During partial drive, the potential is ~100 V.

- There are four stages in the evolution: **1-pinch, 2-driven, 3-decay, 4-partial drive**.
- The peak instantaneous power input reaches ~1 GW in the driven stage.

Toroidal current and magnetic energy evolution from the simulations are similar to results found by CORSICA fits to laboratory observations [Hooper, *et al.*, NF **39**, 863 (1999)] during the partial-drive stage.

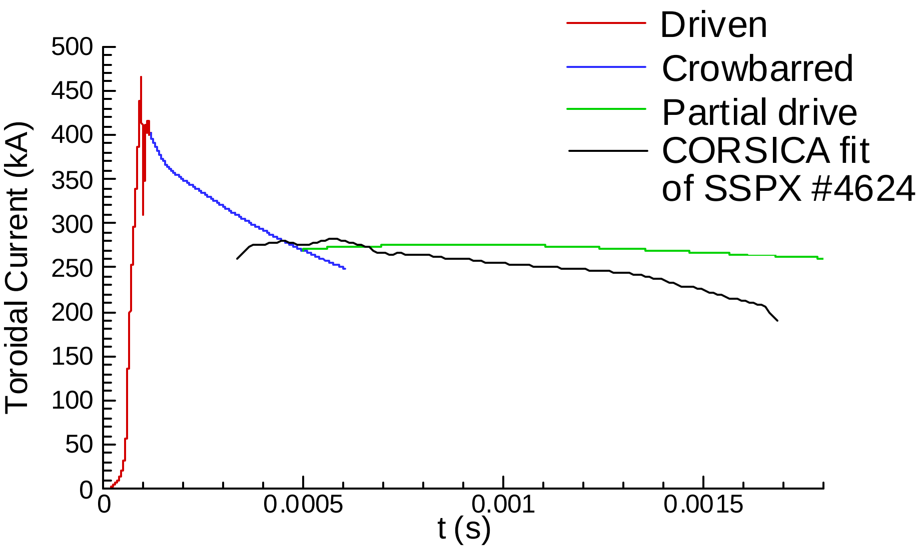

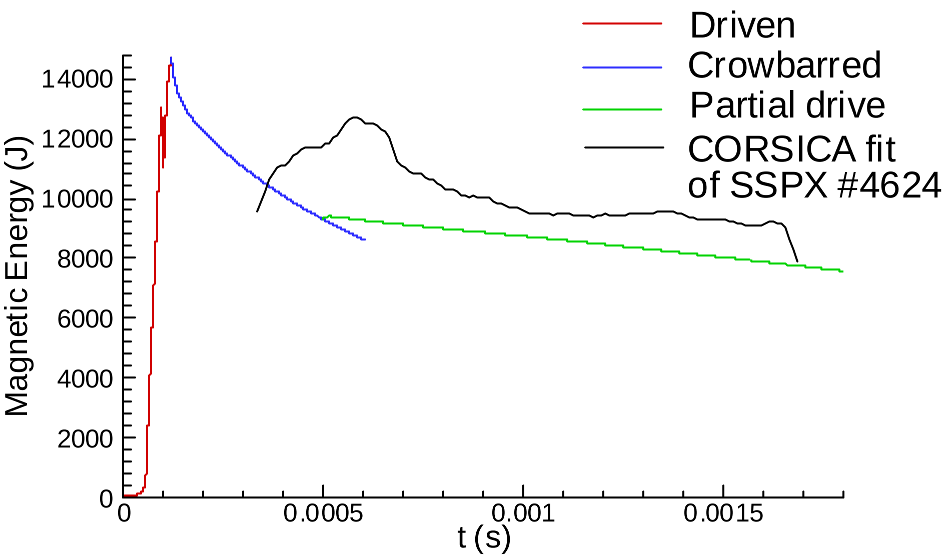

I_{tor} resulting from the series of NIMROD simulations is compared with I_{tor} from CORSICA equilibrium fits of SSPX data.

Simulation and experiment show decreasing magnetic energy after the initial pulse that is slowed by the partial drive.

• During partial drive in the simulation, the injector circuit provides 14 MW of power and the decay of magnetic energy provides and additional 1.4 MW.

<u>Both simulation and experiment show a quiescent phase when partial drive is applied after a brief period of decay.</u>

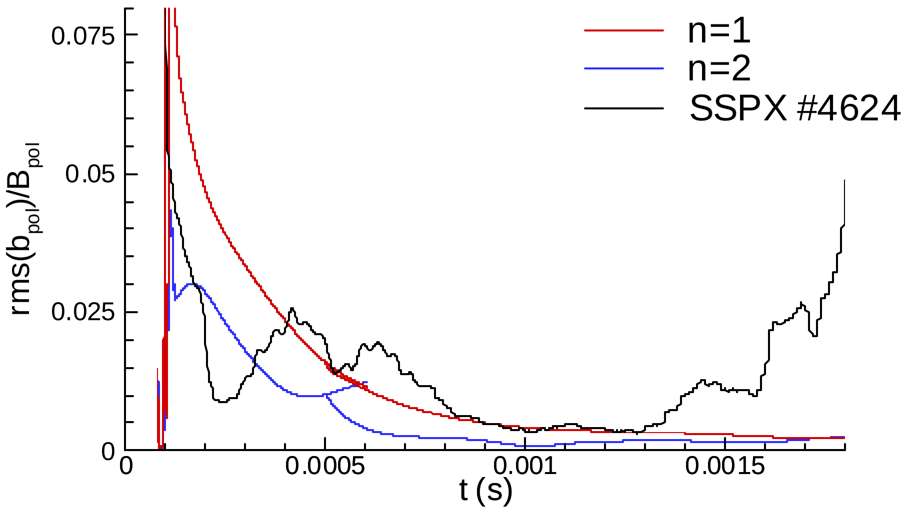

Relative poloidal magnetic field fluctuations at the outboard mid-plane position.

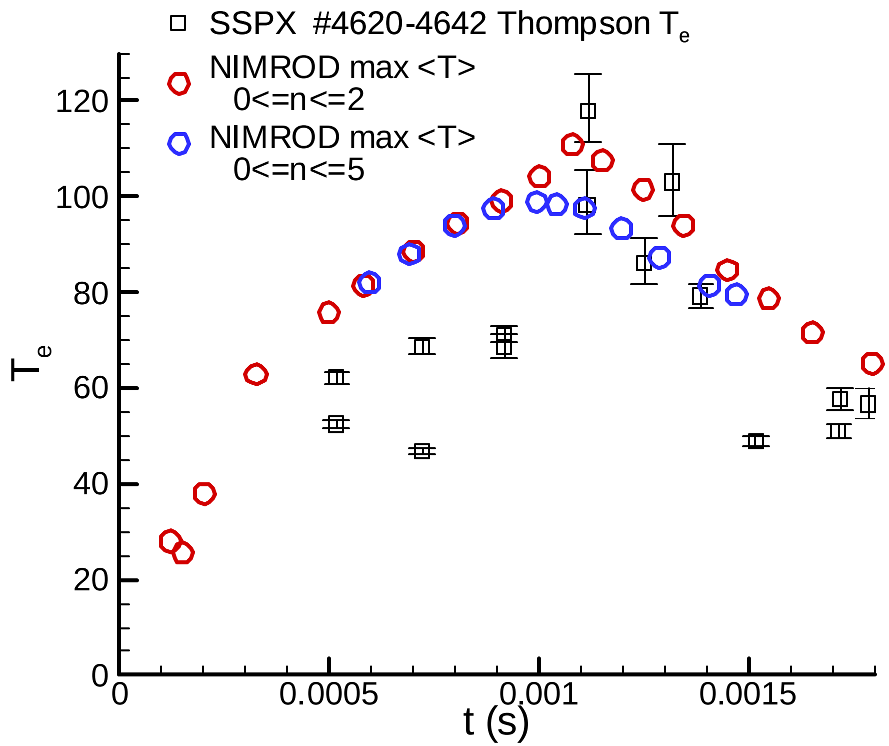

Observed and computed temperatures are highest during the quiescent phase.

- Although conditions are not sustained, partial drive forces fluctuations to smaller amplitude and postpones the emergence of the *n*=2 mode.
- A second partial-drive computation includes all $n \leq 5$ and produces fluctuations at larger *n*-values that reduce *T* late in time.

Four Stages of Evolution

An animation of the numerical results helps distinguish characteristics of the different stages.

- Left side shows axisymmetric parallel current density.
- Right side shows axisymmetric temperature and poloidal flux function.
- Bottom plot shows advancing time and injected current.

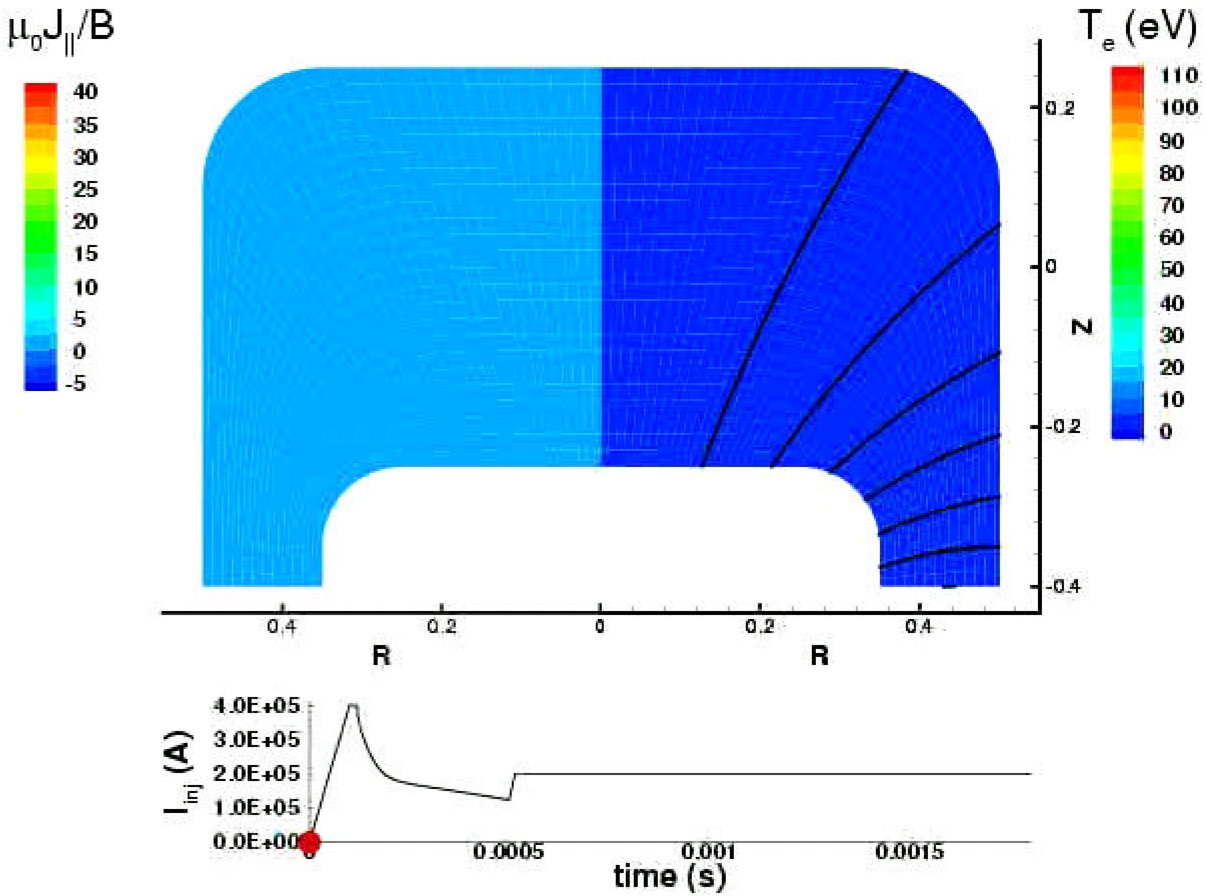

Four Stages of Simulated Evolution: 1-Symmetric Pinch (t<0.08 ms)

• Injected toroidal flux pushes plasma and poloidal flux into the flux-conserver region.

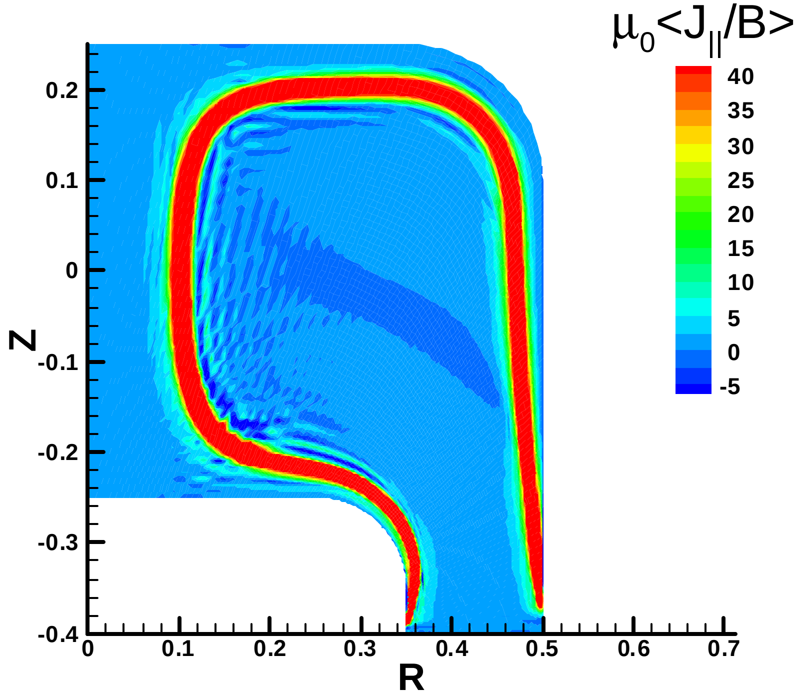

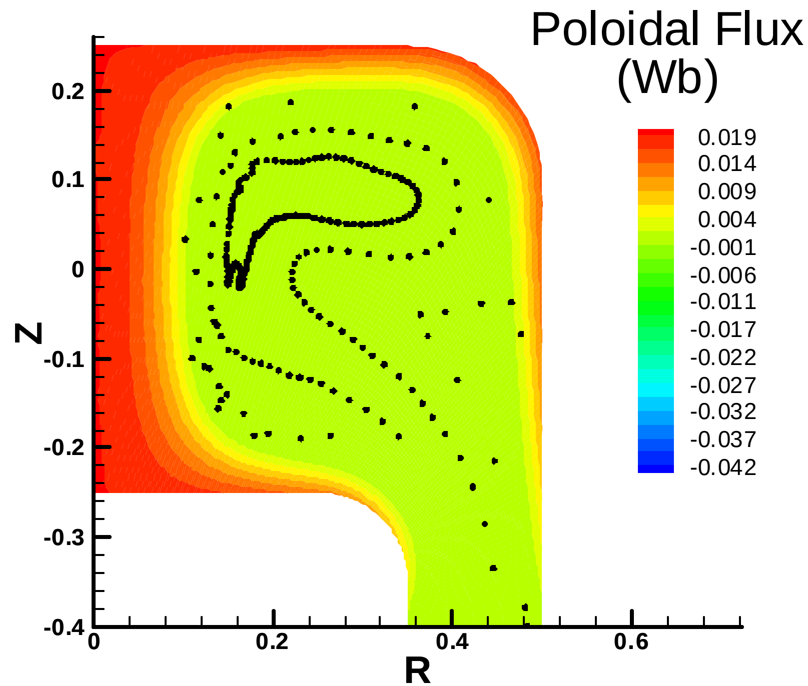

With temperature-dependent resistivity, current is carried by a thin layer until the symmetric distribution becomes MHD unstable.

The vacuum poloidal flux is stretched and compressed, but there is no flux amplification at this stage. The Poincaré plot shows some dynamically formed closed-flux surfaces.

Four Stages of Simulated Evolution: 2-Driven ($0.08 \le t \le 0.12$ ms)

• Similar to 0-*b* simulation results, saturation of the *n*=1 mode leads to redistribution of parallel current through the MHD dynamo effect.

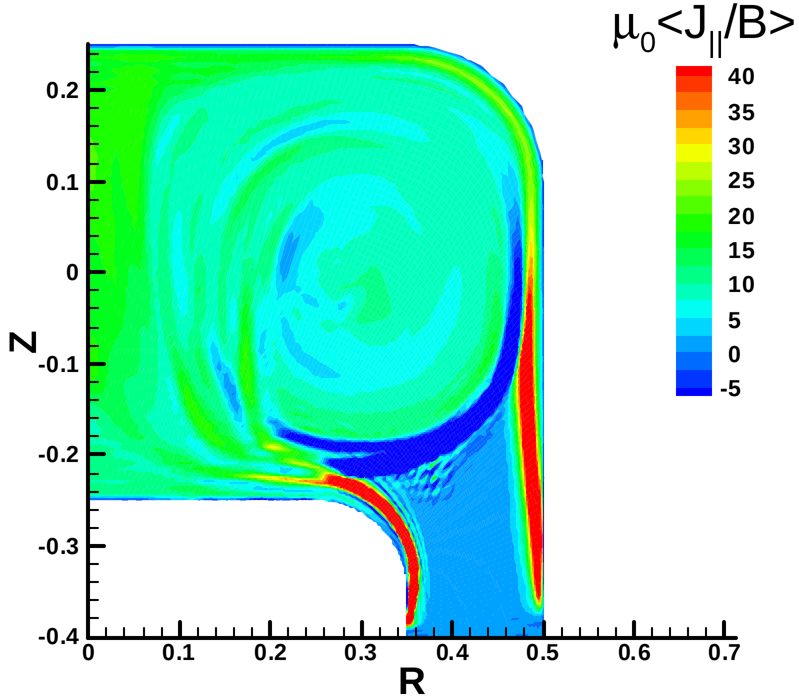

The symmetric component of parallel current density is positive throughout most of the flux conserver.

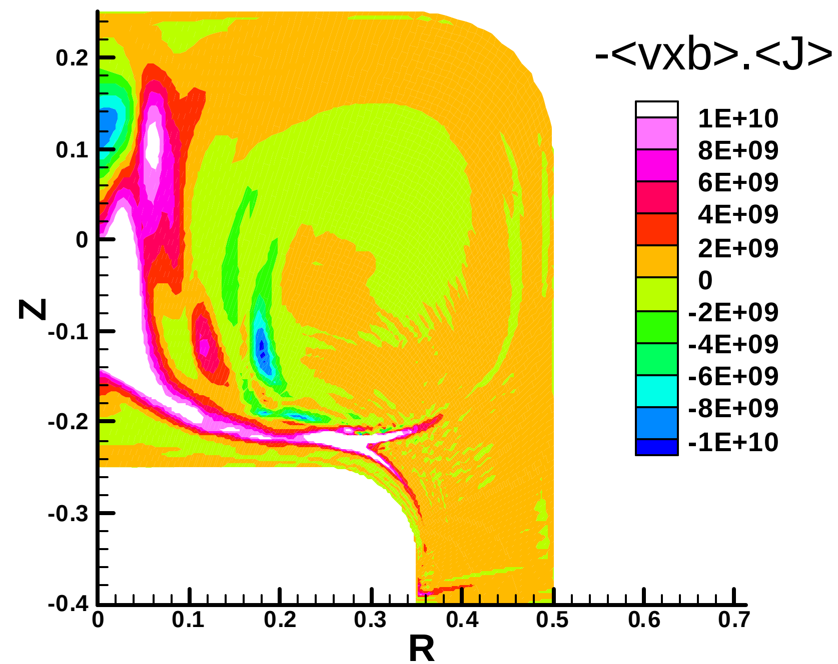

Regions of positive power density transfer energy from the symmetric magnetic field to fluctuations; negative power density drives symmetric current.

• Dynamo electric field was measured in SPHEX, but *n*>1 was thought to represent separate activity [al-Karkhy, *et al*., PRL **70,** 1814 (1993).

Four Stages of Simulated Evolution: 2-Driven ($0.08 \leq t \leq 0.12$ ms)

• Also similar to 0-*b* simulation results, saturation of the n=1 mode (including reconnection) converts toroidal magnetic flux into poloidal magnetic flux.

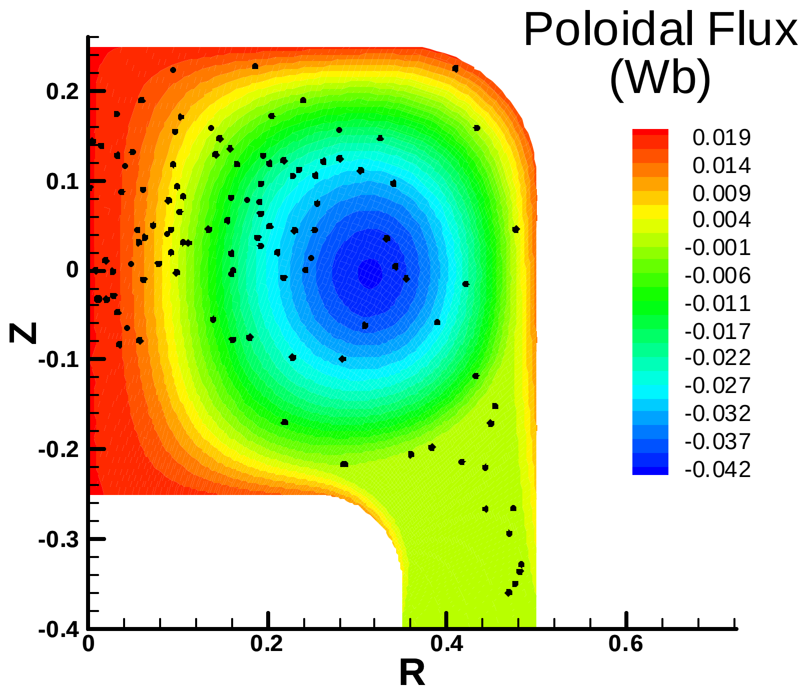

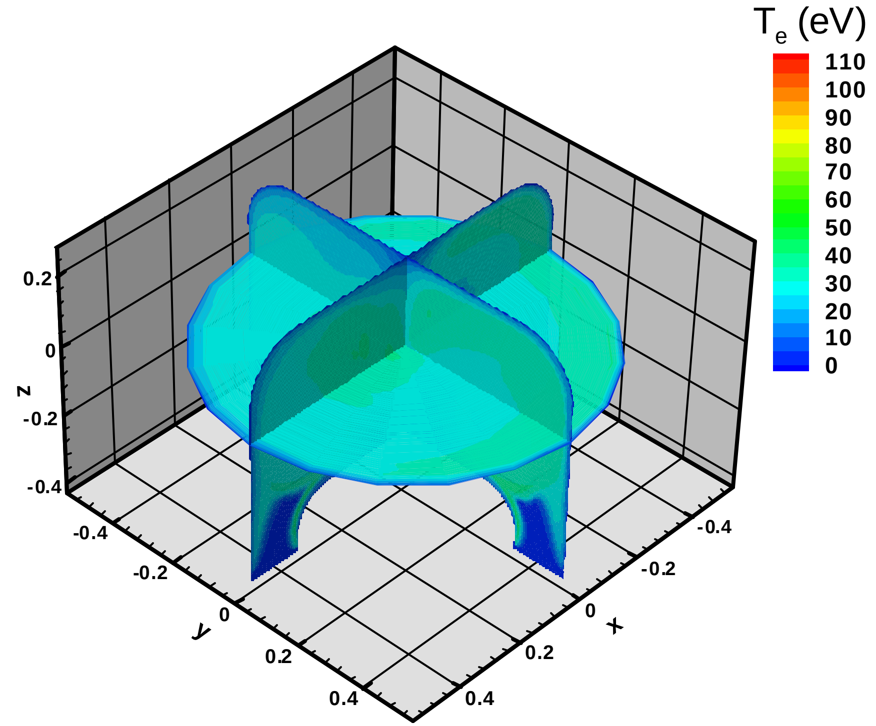

The symmetric component of poloidal magnetic flux has a new minimum value, indicating ~200% flux amplification. However, magnetic field-lines show chaotic scattering.

With chaotic magnetic field-lines, parallel conduction transports heat to the walls, and T is essentially uniform with a maximum of ~35 eV.

• Analytical estimate is ~30 eV. [Hooper, J. Nucl. Materials **278**, 104 (2000).]

Four Stages of Simulated Evolution: 3-Decay ($0.12 \leq t \leq 0.5$ ms)

• With the drive off, temperature on the outer field-lines decreases rapidly, enhancing resistive reconnection and the formation of flux surfaces.

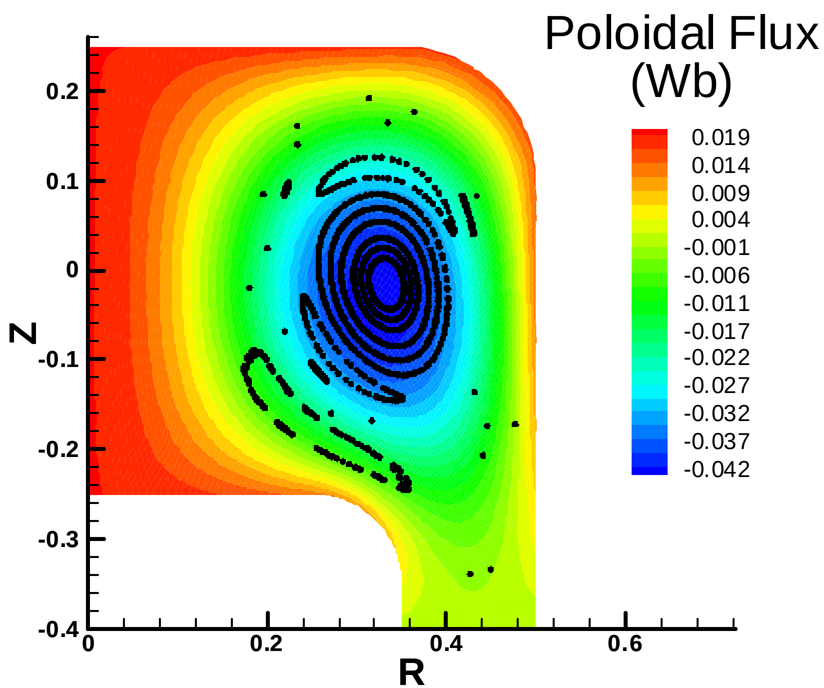

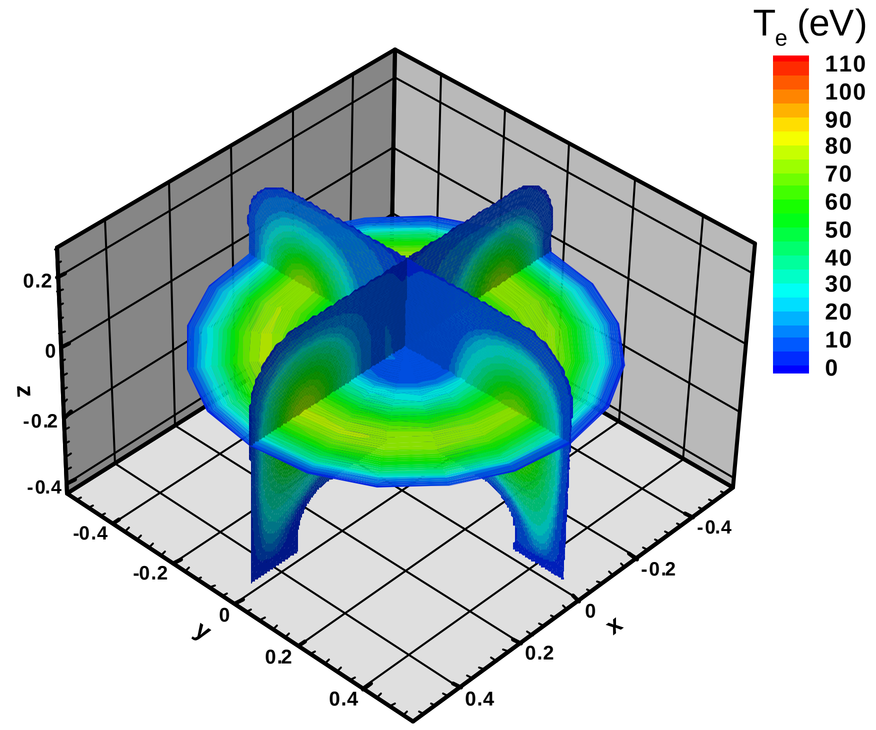

Magnetic fluctuations decay faster than the amplified poloidal flux, producing large closed-flux surfaces.

Energy confinement improves while Ohmic heating continues through magnetic energy decay. At 0.5 ms, the temperature at the magnetic axis reaches 76 eV.

Thermal transport changes character from driven (top row) to decaying conditions (bottom row).

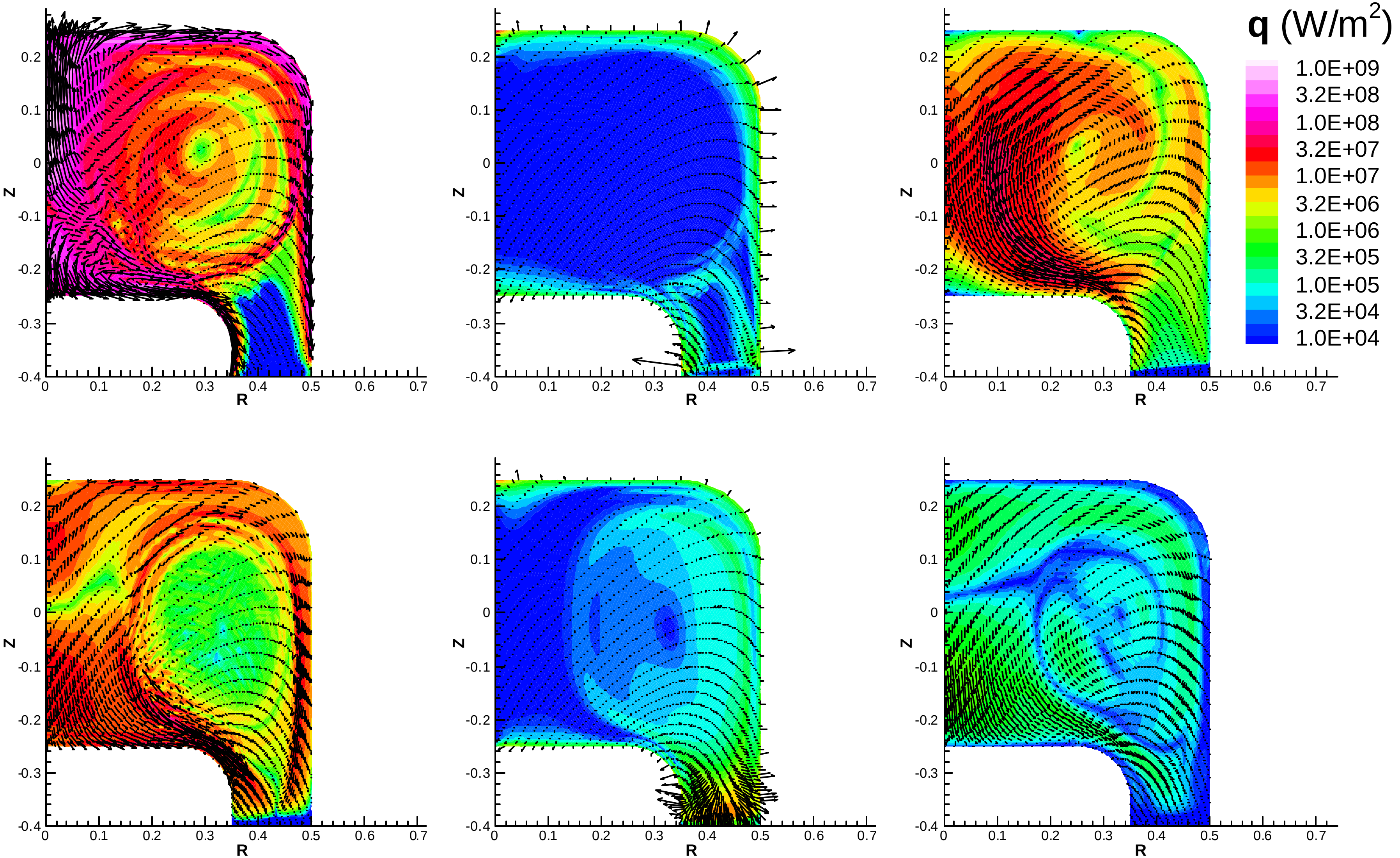

conductive $\langle q_\parallel \mathbf{B}_{pol} \rangle$ conductive $\langle \mathbf{q}_{\perp pol} \rangle$ convective $\langle 2nT\mathbf{V}_{pol} \rangle$

Note the exponential scale for the magnitudes of the three heat vectors.

Four Stages of Simulated Evolution: 4-Partial Drive (0.5 ms≤t)

• With partial drive, the flux surfaces persist longer, and the peak temperature is higher.

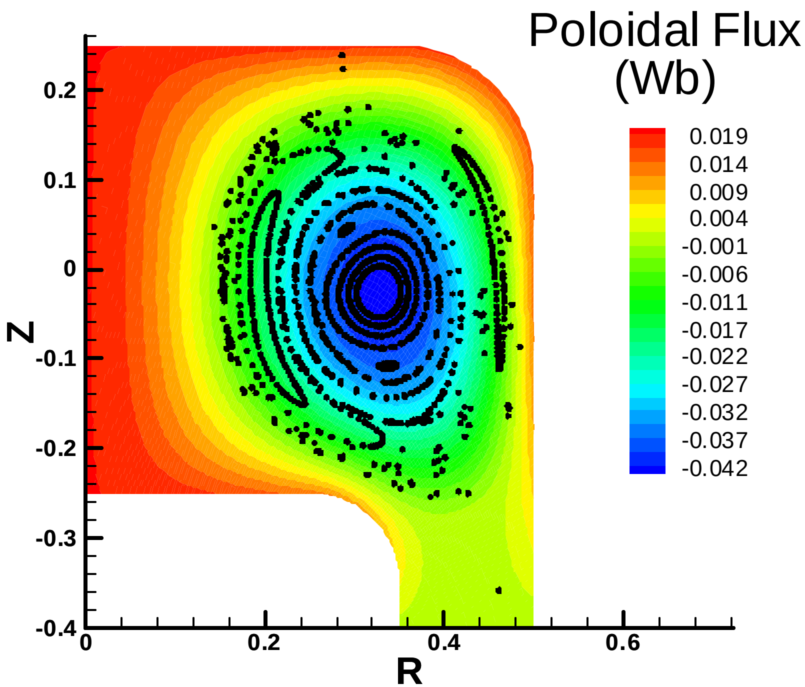

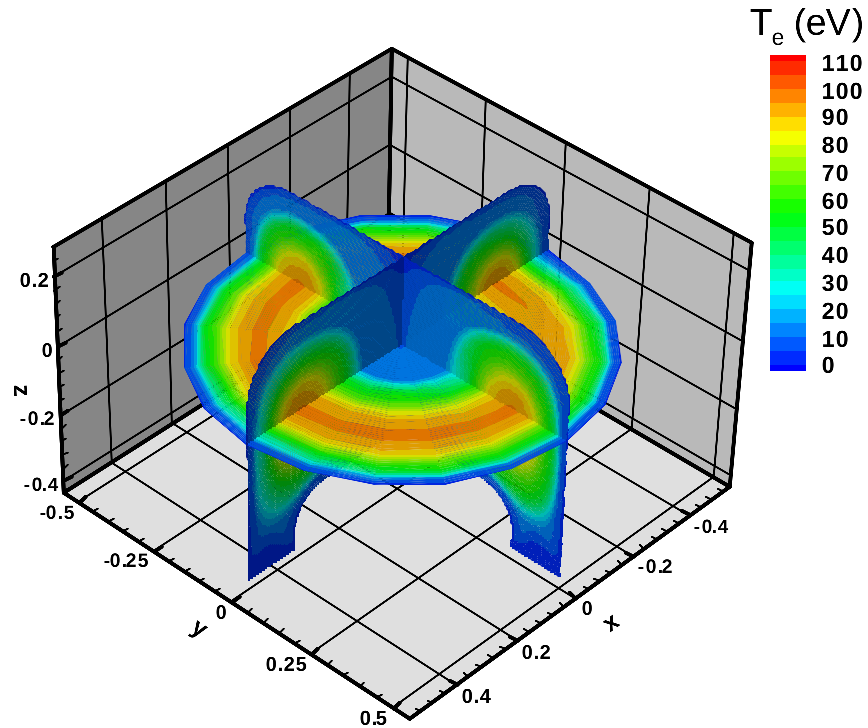

Topologically, the partial drive stage is similar to decay.

The ‘shot’-maximum temperature of 98.8 eV occurs at t=1.0 ms.

• The second drive delays the onset of resonant n=2 activity, and it heats plasma surrounding the flux surfaces.

• The partial-drive simulation with better toroidal resolution (0≤n≤5) produces more resonant MHD activity and a slightly lower maximum temperature.

Safety factor profiles suggest that the improvement from partial drive results from avoiding the *q*=0.5 surface [~Woodruff and McLean, recent].

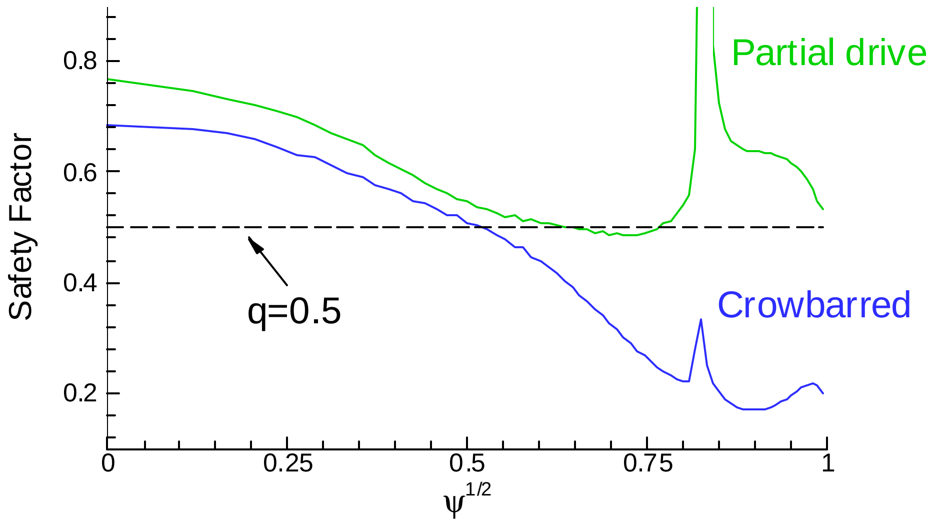

Safety factor profiles at t=1 ms from the partial drive simulation and an extended free decay simulation.

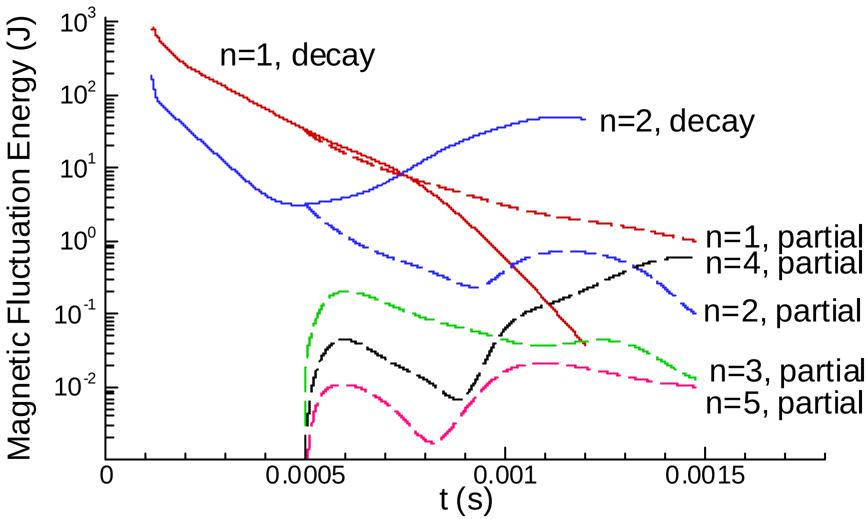

Comparison of magnetic fluctuation energies for free decay and partial drive.

- **By suppressing the n=2 mode, simulations with partial drive achieve twice the internal energy at 1 ms.**
- **Other factors may contribute—further investigation is needed.**

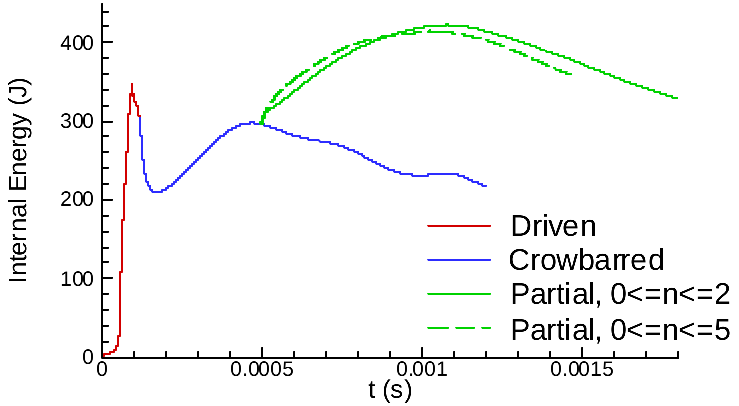

Through further diagnosis of the simulation results, we will be able to characterize factors affecting the *q*-profile evolution and, ultimately, to optimize operation.

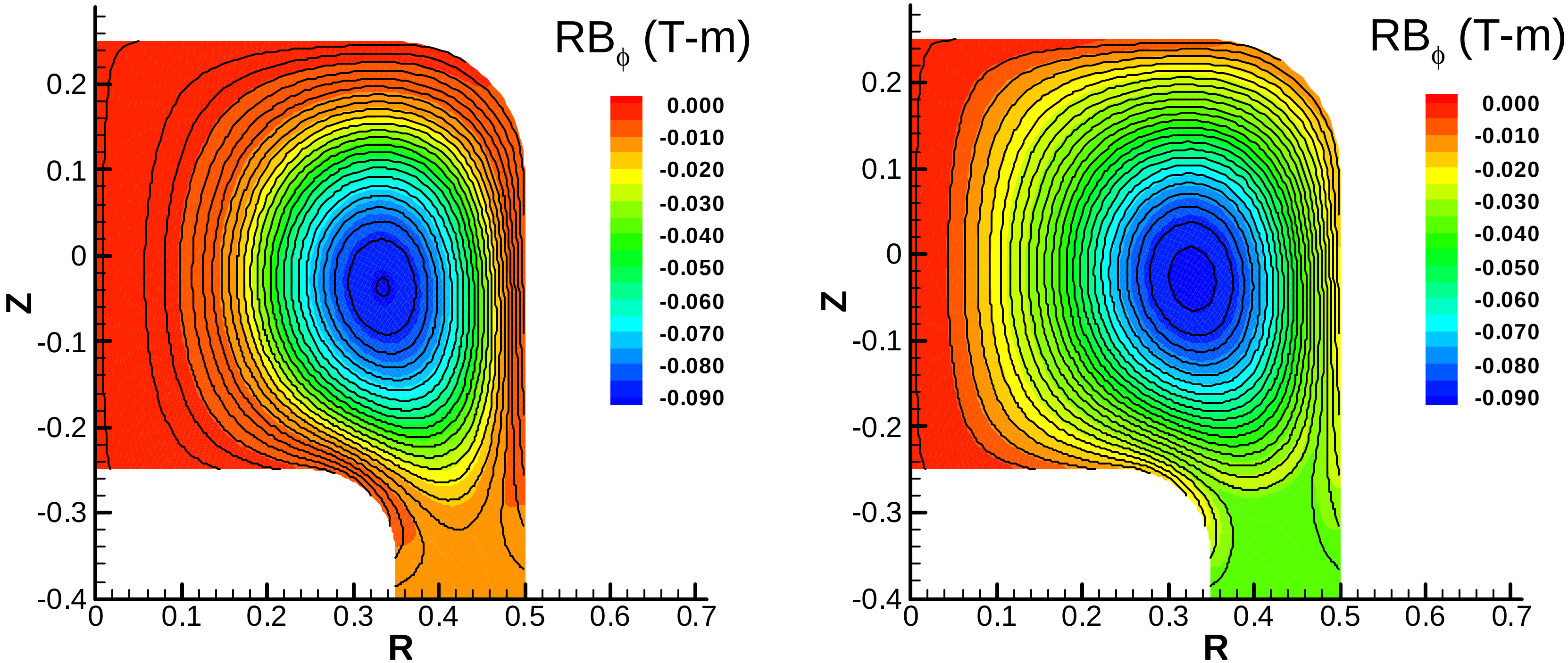

Contours of RB_f with poloidal flux overlaid from the extended free decay simulation (left) and the partial-drive simulation (right) at t=1 ms.

- Pressure from the toroidal field affects poloidal flux shaping (via II' in the Grad-Shafranov equation).
- The partial-drive injector current maintains RB_f at the edge of the amplified-flux region, preventing the minimum q-value from falling below ~0.5.

Driven vs. Partial-Drive Dynamo Activity

• Although the partial-drive stage has half of the injected current as the driven stage, the dynamo power density is two orders of magnitude smaller. [Note the contour-level scales in the following plots.]

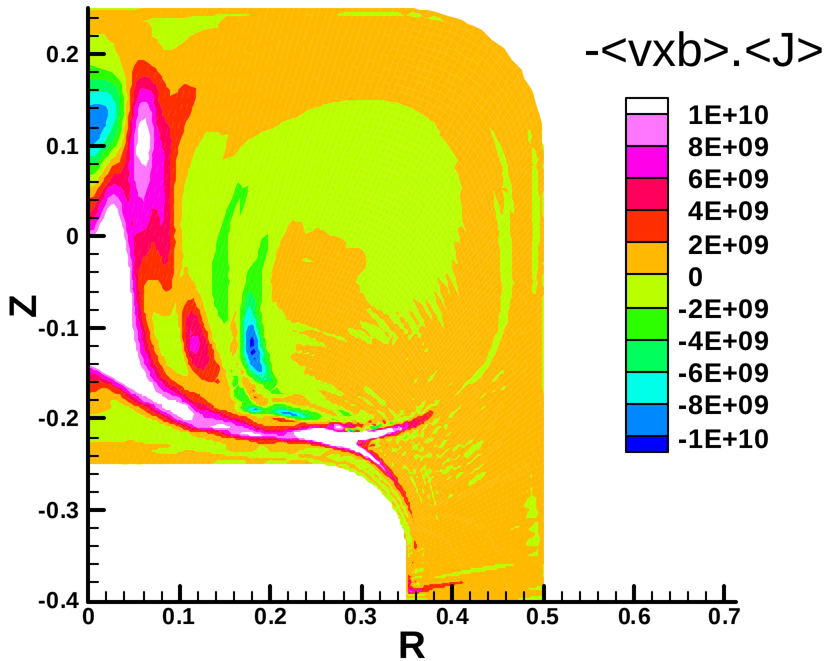

Dynamo power density at t=0.12 ms.

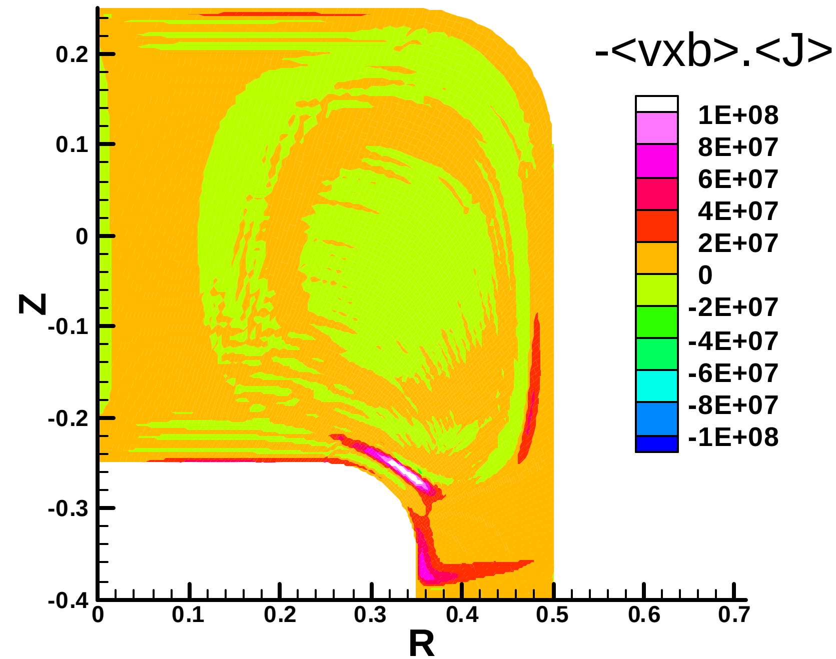

Dynamo power density at t=1.1 ms.

• The ratio of electrical conductivities at the respective temperatures is less than 10.

• At 50 eV the symmetric current would require ~8 ms to decay resistively.

• Partial-drive phase with closed flux surfaces is not representative of sustainment.

Discussion

- An interplay of inductive effects and temperature-dependent transport coefficients produces the low-fluctuation, high-confinement states.
  - The *n*=1 mode of the open-field current channel decays rapidly when the drive is removed—the open-field plasma cools, and the pinch current subsides.
  - Low-resistivity plasma within the hot flux surfaces retains toroidal current associated with the *n*=1-generated poloidal flux.
  - The influence of the MHD activity on the magnetic topology during drive and decay are consistent with earlier 0-*b* simulation results (Finn, *et al.*, PRL **85**, 4538, 2002 and Sovinec, *et al.*, PoP **8**, 475, 2001).
- The realistic parameters and collisional temperature dependencies make the MHD results quantitatively consistent with SSPX results:
  - Temperature evolution
  - Magnetic fluctuations of ~1 % during partial drive
  - Magnetic energy decay during partial drive
- The resonant fluctuations during partial should be analyzed with respect to their impact on confinement and not as a mechanism for current drive.
- Simulation results indicate that current-profile relaxation (flux amplification) and self-organization (formation of closed-flux surfaces) are distinct processes.

Conclusions

- Evolving the complete system with temperature-dependent transport coefficients allows us to assess confinement quality during different stages of spheromak operation.
- Transients play a crucial role; thus, modeling injector current programming is necessary for detailed comparison of theory and experiment.
- Relating the 0-*b* simulation results to the recent results *and* from the comparison of the experimental observations with the simulations, we see that only the initial phase of the standard two-stage SSPX operation has the characteristics of full sustainment.
- The success of partial drive provides optimism for tailoring pulsed spheromak operation.

Acknowledgments

- Harry McLean: SSPX data
- SSPX experimental group and LLNL theory group: many helpful discussions
- Ken Fowler: relevance of collisional closures
- John Finn, Diego del-Castillo-Negrete: collaboration on 0-*b* MHD studies
- NIMROD Team: code development collaboration